19. Mechanism of Local Earthquakes in Kwantô Region, Japan, Derived from the Amplitude Relation of P and S Waves.

By Takeshi MIKUMO,*

Disaster Prevention Research Institute, Kyoto University.

1. Introduction

The study of earthquake mechanism has rapidly been developed on both theoretical and observational sides by many seismologists, since T. Shida (1917) discovered a systematic pattern of quadrant type for dilatation and compression of first motions of longitudinal waves in a Japanese earthquake. Up to the present, hypotheses have been given from various standpoints on the earthquake mechanism; that is, from what causes stresses arise and strain energies are accumulated in the crust or the mantle of the earth, and by what processes the energies are suddenly released and seismic waves radiated. Nakano (1923) and Matuzawa (1926) first introduced, as a model of focus, an idea of concentrated body forces acting at a point in an infinite elastic medium and calculated theoretically the field of displacement due to the sources. Nowadays, there are two prevailing hypotheses relating to the focal mechanism which are simplified by force systems applied to an equivalent focus.

The one is analytically represented by two equal and opposite forces or a single couple with moment, indicating motion along a fault. The so-called fault-plane solution means determining an orientation of the fault and the motion direction from the first motion of P waves at many stations distributed over the earth, by a stereographic projection. The method is based on Nakano's theory and was established first by Byerly (1928). By this technique, however, the fault plane and the auxiliary plane perpendicular to the former cannot be distinguished from each other, so he suggested later (1949) a method using also S wave data. Hodgson (1951, 1953, 1957) and Ritsema (1957, 1959) have developed Byerly's method on the same basis and determined the mechanism of

---

* Visiting Research Fellow at the Earthquake Research Institute (Oct., 1961—March, 1962).

many earthquakes.   Keylis-Borok (1956, 1957, 1960) also derived the
displacement field of body waves caused by similar force systems, and
used distribution of the sign of SV and SH waves as well as of P
waves in determination of source mechanism, proposing the use of
amplitude ratios of the waves.

The other is the force system of double couples with moment, being
perpendicular to each other, which is equivalent to two sets of
compressional and tensile stresses of equal magnitude working at right
angles at the focus.   Honda (1934, 1957) presented a focal mechanism
with a radial force of harmonic type acting on the surface of a model
sphere, and discussed (1957) the amplitudes of both P and S waves.
Kawasumi (1933) dealt with a similar type of mechanism in the form
of a particular solution of wave equation.   Vvedenskaya (1959, 1960)
calculated the displacements of waves radiated by faulting, like a strike-
slip fault in a limited area, by applying the dislocation theory to the
problem.   Moreover, Knopoff and Gilbert (1959, 1960) recently studied
displacement patterns due to sudden dislocation along a fault plane,
especially those in bilateral faulting and those in the case of discontinuity
of displacement.   Displacement fields resulting from these three focal
models are quite analogous to those of the double couple point source.

The above two types of force systems each give an identical
quadrant distribution of P waves.   Therefore, we cannot judge which
of them better represents the real focus solely from observation of P
waves.   The problem may be solved by the use of reliable data of S
waves, since the pattern of the first motion of S differs for the two
cases.   This has been intensively studied not only by the above authors
but by Adams, Stauder (1958, 1959, 1960) and others.

On the other hand, another mechanism of cone-type was proposed
by some Japanese seismologists from different points of view, as reviewed
by the present author himself (1959).   Ishimoto (1932) proposed a focal
model composed of single and quadruple sources, and Kawasumi (1933)
investigated the amplitude distribution in this type.   A similar type of
mechanism was studied by Inouye (1936), Takagi (1953), Usami and
Hirono (1958), in which the displacements were obtained for many types
of forces applied on the surface of spherical or spheroidal cavity.   Ingram
recently investigated (1960) a system of forces consisting of three coules
without moment, which is included in the general theory of Keylis-Borok
(1957).   In these cases, the distribution of condensation and rarefaction
of P waves is not separated by two orthogonal planes, but by a set of

conical surfaces with its vertex at the focus.

As mentioned above, various theoretical models representing the focal mechanism have been presented, but their appropriateness should be attested by observation. The observational studies consist mainly in the line on which nodal planes are tentatively estimated from distribution of the first motion directions of P and S waves and confirmed in some cases by the wave amplitudes themselves. Most of the studies of this kind have been associated with great earthquakes and not with earthquakes of small magnitude. This may be by reason of the difficulty of applying a similar technique to the latter case owing to a lack of sufficient data over a wide area. However, the question wether the mechanism of these earthquakes may be identically solved or whether it may depend upon the earthquake magnitude, its focal depth and some other factors, seems to remain unanswered. It is an interesting problem from this standpoint to investigate the mechanism of very small earthquakes, such as of local shocks or aftershocks in seismically active regions, and the relationship, if it exists, with that of greater earthquakes that occurred in the same area. To approach the problem the writer (1959) has studied the local earthquake mechanism in Wakayama District. Now, for the same purpose, we shall study the focal mechanism of minor earthquakes taking place in the southern Kwantô region, Japan.

2. Theory

In the present study, instead of the usual method mentioned above, we shall introduce a way of deducing a focal mechanism from the amplitude relations of body waves observed at a few stations. Assuming the type of mechanism or the applied force system to be the three prevailing models, namely, a single couple, double couples and cone-type respectively, the expected field of displacement amplitudes of P, SV and SH waves will be calculated in convenient forms for practical use of observed data. The theoretical amplitude ratios in comparison with observed ones on which the effects of crustal structure are taken into account, lead to a determination of dynamic parameters of the focus. The method using amplitude ratios was suggested by Byerly, Stauder (1958) and Keylis-Borok (1957), and sometimes adopted successfully in a practical research by Soviet seismologists (Keylis-Borok, 1957; Vvedenskaya, 1960). This may be valid for our present purpose. The respective mean errors in a statistical average of the estimated values

will serve to identify what type of mechanism is most reasonably fitted to the real source.

(1) *Single couple*

We shall first consider a single couple of forces $+K(t)/\delta s$ and $-K(t)/\delta s$ acting on the points A and A', each distance from the focus being $\delta s/2$. Let us suppose an orthogonal co-ordinate of the left-hand side system with its origin at the focus, as shown in Fig. 1, and let the direction cosines of the forces be $\pm l$, $\pm m$, $\pm n$, and those of the line elements OA and OA' $\pm\lambda$, $\pm\mu$, $\pm\nu$, repectively. The displacement components (u_x, u_y, u_z) due to the forces at any point $P(x, y, z)$ in an infinite elastic medium, being distant from the source, are expressed as follows, in the limiting case when $\delta s \to 0$. (Nakano, 1923).
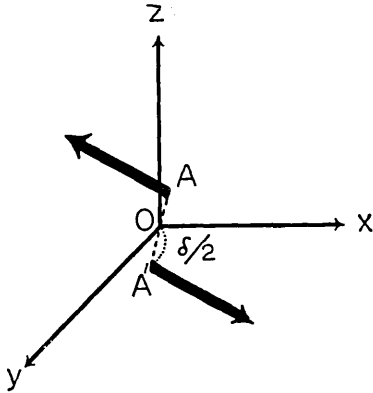
Fig. 1. *A single couple.*

$$u_x = u_{ax} + u_{bx} , \quad u_y = u_{ay} + u_{by} , \quad u_z = u_{az} + u_{bz} ,$$

and

$$u_{ax} = \frac{1}{4\pi\rho a^3 r^4}(\lambda x + \mu y + \nu z)(lx + my + nz)x \cdot K'(t - r/a)$$

$$u_{ay} = \frac{1}{4\pi\rho a^3 r^4}(\lambda x + \mu y + \nu z)(lx + my + nz)y \cdot K'(t - r/a)$$

$$u_{az} = \frac{1}{4\pi\rho a^3 r^4}(\lambda x + \mu y + \nu z)(lx + my + nz)z \cdot K'(t - r/a)$$

$$u_{bx} = \frac{-1}{4\pi\rho b^3 r^4}(\lambda x + \mu y + \nu z)[(lx + my + nz)x - lr^2] \cdot K'(t - r/b)$$

$$u_{by} = \frac{-1}{4\pi\rho b^3 r^4}(\lambda x + \mu y + \nu z)[(lx + my + nz)y - mr^2] \cdot K'(t - r/b)$$

$$u_{bz} = \frac{-1}{4\pi\rho b^3 r^4}(\lambda x + \mu y + \nu z)[(lx + my + nz)z - nr^2] \cdot K'(t - r/b)$$

(1)

where r is the distance from the origin, ρ the density of the medium, a and b the progagation velocities of P and S waves. The above two kinds of terms are associated with the emitted P and S waves respectively.

The displacements can be rewritten as u_r, u_θ and u_φ in the spherical

co-ordinate. That is,

$$u_r = (u_x \cos \varphi + u_y \sin \varphi) \sin \theta + u_z \cos \theta$$
$$u_\theta = (u_x \cos \varphi + u_y \sin \varphi) \cos \theta - u_z \sin \theta \qquad (2)$$
$$u_\varphi = -u_x \sin \varphi + u_y \cos \varphi$$

After algebraic calculation, they are expressed as ;

$$u_r = \frac{A_p}{r} (\lambda \sin \theta \cos \varphi + \mu \sin \theta \sin \varphi + \nu \cos \theta)$$
$$\times (l \sin \theta \cos \varphi + m \sin \theta \sin \varphi + n \cos \theta)$$
$$u_\theta = \frac{A_s}{r} (\lambda \sin \theta \cos \varphi + \mu \sin \theta \sin \varphi + \nu \cos \theta)$$
$$\times (l \cos \theta \cos \varphi + m \cos \theta \sin \varphi - n \sin \theta) \qquad (3)$$
$$u_\varphi = \frac{-A_s}{r} (\lambda \sin \theta \cos \varphi + \mu \sin \theta \sin \varphi + \nu \cos \theta)$$
$$\times (l \sin \varphi - m \cos \varphi)$$

where

$$A_p = \frac{K'(t-r/a)}{4\pi\rho a^3}, \qquad A_s = \frac{K'(t-r/b)}{4\pi\rho b^3}$$

(Byerly and Stauder, 1958 ; Ichikawa, 1959).

We note that u_r takes a positive sense for motion away from epicentre, u_θ increases for motion up and toward epicentre and u_φ for clockwise motion looking from epicentre to station.

In a special case when the x-axis is taken along the motion direction and the z-axis along OA, that is, when $l=1$, $m=n=0$ and $\lambda=\mu=0$, $\nu=1$, Eqs. (1) and (3) are simplified in the following.

$$u_a = \frac{xz}{4\pi\rho a^3 r^3} K'(t-r/a) , \qquad u_b = \frac{z\sqrt{r^2-x^2}}{4\pi\rho b^3 r^3} K'(t-r/b) \qquad (4)$$

$$u_r = \frac{A_p}{r} \frac{1}{2} \sin 2\theta \cos \varphi$$
$$u_\theta = \frac{A_s}{r} \cos^2 \theta \cos \varphi \qquad (5)$$
$$u_\varphi = -\frac{A_s}{r} \cos \theta \sin \varphi .$$

The former equations have the identical form as derived by Keylis-Borok (1957).

We shall here introduce a co-ordinate system $(\bar{x}\,\bar{y}\,\bar{z})$ convenient for
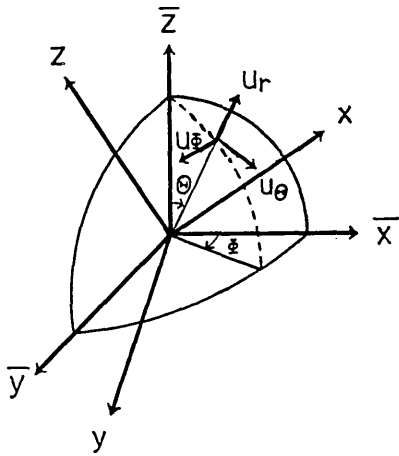
Fig. 2.

the use of observed data. Let the $\bar{x}$-axis be directed north, the $\bar{y}$ east and the $\bar{z}$ upward, as indicated in Fig. 2. We denote the emergent angle of seismic ray at the focus by Θ, and the azimuth of a station relating to epicentre by Φ, which is measured clockwise from northward. The displacement field (u_r, u_Θ, u_Φ) referring to this system can immediately be obtained if we transform θ to Θ and φ to Φ in Eq. (3). The componenents u_r, u_Θ and u_Φ correspond to the amplitudes of P, SV and SH waves in a homegeneous earth, respectively.

Let the angle of inclination of motion direction to horizontal surface be ψ, and the azimuth of horizontal trace of the direction be β, we then find that $l = \cos\psi\cos\beta$, $m = \cos\psi\sin\beta$, $n = \sin\psi$. If we put the amplitude ratios for the three types of waves in the form ;

$$h_1 = u_r/u_\Theta, \quad h_2 = u_r/u_\Phi, \quad h_3 = u_\Theta/u_\Phi \quad \text{and} \quad k = (b/a)^3, \quad (6)$$

the following equations can be derived from Eq. (3),

$$\left. \begin{aligned} h_2 &= -k\frac{\sin\Theta\cos(\Phi-\beta)+\cos\Theta\tan\psi}{\sin(\Phi-\beta)} \\ h_3 &= -\frac{\cos\Theta\cos(\Phi-\beta)-\sin\Theta\tan\psi}{\sin(\Phi-\beta)} \end{aligned} \right\} \quad (7)$$

Θ and Φ will be determined when hypocentre is located, and h_2 and h_3 will be measurable on a recorded seismogram with some corrections. The two unknown factors, β and ψ, can therefore be solved from Eq. (7), That is,

$$\left. \begin{aligned} \sin(\Phi-\beta) &= \frac{k}{\sqrt{k^2 + (h_2\sin\Theta + kh_3\cos\Theta)^2}} \\ \tan\psi &= \frac{kh_3 + (h_2\sin\Theta + kh_3\cos\Theta)\cos\Theta}{\sin\Theta\sqrt{k^2 + (h_2\sin\Theta + kh_3\cos\Theta)^2}}. \end{aligned} \right\} \quad (8)$$

Another form of solution is as follows, if we put $\tan\beta = X$ and $\sec\beta\tan\psi = Y$;

$$X=\frac{A(1-BM)+N}{1-BM-AN} , \quad Y=\frac{BCM}{1-BM-AN} \tag{9}$$

where

$$A=\tan\varPhi , \quad B=\cot\varTheta\sec\varPhi , \quad C=\tan\varTheta\sec\varPhi ,$$

$$M=(2-K_1)/(B+C) , \quad N=K_2=2k\sin\varTheta/h_2 , \quad K_1=2k\tan\varTheta/h_1 .$$

The latter solution was derived for the sake of comparison with that in the other mechanisms. Theoretically it may be possible to determine the motion direction or the plane $lx+my+nz=0$ from data at a single station, assuming this type of mechanism. But the determination of the other plane requires observation at another station.

(2) Double couples

We shall next consider double couples of forces $\pm K(t)/\partial s$ acting respectively at the points A, A' and B, B'. Let the direction cosines of the second couple of forces be $\pm\lambda$, $\pm\mu$, $\pm\nu$ in accordance with those of the first line elements OA and OA' which were shown in Fig. 1, and let the direction cosines of the second line elements OB and OB' be $\pm l$, $\pm m$, $\pm n$ with those of the first couple, as illustrated in Fig. 3. The displacement components at a large distance from the origin, analongous to Eq. (1), are expressed in the following, by combination of the respective components in the single couple case ;
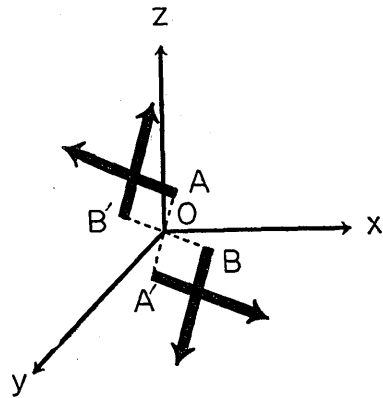

Fig. 3. Double couples.

$$u_{ax}=\frac{2}{4\pi\rho a^3 r^4}(\lambda x+\mu y+vz)(lx+my+nz)x\cdot K'(t-r/a)$$

$$\left.\begin{aligned}
u_{bx}=\frac{-1}{4\pi\rho b^3 r^4}[(\lambda x+\mu y+\nu z)\{(lx+my+nz)x-lr^2\} \\
+(lx+my+nz)\{(\lambda x+\mu y+vz)x-\lambda r^2\}]\cdot K'(t-r/b) \\
\text{etc.}
\end{aligned}\right\} \tag{11}$$

The displacements can be rewritten in the spherical co-ordinate as follows ;

$$
\left.\begin{aligned}
u_r =&\, 2\frac{A_p}{r}(\lambda \sin\theta \cos\varphi + \mu \sin\theta \sin\varphi + \nu \cos\theta) \\
&\times (l \sin\theta \cos\varphi + m \sin\theta \sin\varphi + n \cos\theta) \\
u_\theta =&\, \frac{A_s}{r}[(\lambda \sin\theta \cos\varphi + \mu \sin\theta \sin\varphi + \nu \cos\theta) \\
&\times (l \cos\theta \cos\varphi + m \cos\theta \sin\varphi - n \sin\theta) \\
&+ (l \sin\theta \cos\varphi + m \sin\theta \sin\varphi + n \cos\theta) \\
&\times (\lambda \cos\theta \cos\varphi + \mu \cos\theta \sin\varphi - \nu \sin\theta)] \\
u_\varphi =&\, -\frac{A_s}{r}[(\lambda \sin\theta \cos\varphi + \mu \sin\theta \sin\varphi + \nu \cos\theta)(l \sin\varphi - m \cos\varphi) \\
&+ (l \sin\theta \cos\varphi + m \sin\theta \sin\varphi + n \cos\theta)(\lambda \sin\varphi - \mu \cos\varphi)]\ .
\end{aligned}\right\} \quad (12)
$$

In a special case when the x- and z-axes are taken along the positive force directions of two couples, Eqs. (11) and (12) can be simplified to;

$$
\left.\begin{aligned}
u_a &= \frac{2xz}{4\pi\rho a^3 r^3}\cdot K'(t-r/a)\ , \\
u_b &= \frac{\sqrt{z^2(r^2-x^2)+x^2(r^2-z^2)}}{4\pi\rho b^3 r^3}\cdot K'(t-r/b)
\end{aligned}\right\} \quad (13)
$$

$$
\left.\begin{aligned}
u_r &= \frac{A_p}{r}\sin 2\theta \cos\varphi \\
u_\theta &= \frac{A_s}{r}\cos 2\theta \cos\varphi \\
u_\varphi &= -\frac{A_s}{r}\cos\theta \sin\varphi
\end{aligned}\right\} \quad (14)
$$

The latter equations are identical with that derived by Honda (1934). Comparing Eqs. (12), (13) and (14) with Eqs. (3), (4) and (5) in a single couple, respectively, we find that the amplitude distributions of the P waves are quite similar to each other.

When we introduce the geographical co-ordinate as in the preceding section, the displacement amplitudes of P, SV and SH waves can be obtained by replacing θ with Θ and φ with Φ in Eq. (12). Let the plunge of motion directions of two kinds of forces be ψ_1 and ψ_2, and the azimuth of the horizontal traces of them be β_1 and β_2, we then find that $l=\cos\psi_1\cos\beta_1$, $m=\cos\psi_1\sin\beta_1$, $n=\sin\psi_1$ and $\lambda=\cos\psi_2\cos\beta_2$, $\mu=\cos\psi_2\sin\beta_2$, $\nu=\sin\psi_2$. The amplitude ratios, h_1 and h_2, are related to the two known values Θ and Φ and four unknown factors β_1, β_2, ψ_1 and ψ_2 in the

following form ;

$$
\left.
\begin{aligned}
2\frac{k}{h_1} &= \frac{\cos\Theta\,\cos(\Phi-\beta_1)-\sin\Theta\,\tan\psi_1}{\sin\Theta\,\cos(\Phi-\beta_1)+\cos\Theta\,\tan\psi_1} \\
&\quad+\frac{\cos\Theta\,\cos(\Phi-\beta_2)-\sin\Theta\,\tan\psi_2}{\sin\Theta\,\cos(\Phi-\beta_2)+\cos\Theta\,\tan\psi_2} \\
-2\frac{k}{h_2} &= \frac{\sin(\Phi-\beta_1)}{\sin\Theta\,\cos(\Phi-\beta_1)+\cos\Theta\,\tan\psi_1} \\
&\quad+\frac{\sin(\Phi-\beta_2)}{\sin\Theta\,\cos(\Phi-\beta_2)+\cos\Theta\,\tan\psi_2}.
\end{aligned}
\right\}
\quad (15)
$$

If we put $\tan\beta_i=X_i$ and $\sec\beta_i\tan\psi_i=Y_i$ $(i=1, 2)$, Eq. (15) may be written as follows ;

$$
\left.
\begin{aligned}
M_j &= \frac{Y_1}{1+A_jX_1+B_jY_1}+\frac{Y_2}{1+A_jX_2+B_jY_2} \\
N_j &= \frac{X_1-A_j}{1+A_jX_1+B_jY_1}+\frac{X_2-A_j}{1+A_jX_2+B_jY_2}
\end{aligned}
\right\}
\quad (16)
$$

where

$$
\begin{aligned}
&A_j=\tan\Phi_j, \quad B_j=\cot\Theta_j\sec\Phi_j, \quad C_j=\tan\Theta_j\sec\Phi_j, \\
&M_j=(2-K_{1j})/(B_j+C_j), \qquad N_j=K_{2j}=2k\sin\Theta_j/h_{2j}, \\
&K_{1j}=2k\tan\Theta_j/h_{1j}.
\end{aligned}
$$

The four unknowns X_1, X_2, Y_1 and Y_2 may be solved in principle from Eq. (16), making use of the data at two stations.

If we assume, however, the two couples intersecting perpendicularly to each other, the following condition holds, $l\lambda+m\mu+n\nu=0$ or $X_1X_2+Y_1Y_2=-1$. Substituting X_2 and Y_2 for X_1 and Y_1 from Eq. (16) into the above condition, and rearranging them, we have a quadratic equation ;

$$
\left.
\begin{aligned}
Y_1^2+P_j(X_1)Y_1+Q_j(X_1)&=0 \\
P_j(X_1)=u_jX_1+v_j, \qquad Q_j(X_1)&=\alpha_jX_1^2+\beta_jX_1+\gamma_j
\end{aligned}
\right\}
\quad (17)
$$

where

$$
\begin{aligned}
&u_j=(b_j+p_j)/q_j, \quad v_j=(g_j+r_j)/q_j, \\
&\alpha_j=a_j/q_j, \quad \beta_j=(c_j+f_j)/q_j, \quad \gamma_j=h_j/q_j, \\
&a_j=A_jD_j-B_jD_j, \quad b_j=B_jD_j, \quad c_j=D_j, \\
&f_j=A_jE_j, \quad g_j=B_jE_j, \quad h_j=E_j-B_jC_j, \\
&p_j=A_jB_jC_jM_j, \quad q_j=-B_jC_j(1-B_jM_j), \quad r_j=B_jC_jM_j,
\end{aligned}
$$

$$D_j = A_j(2 - B_j M_j) + N_j, \quad E_j = 2 - B_j M_j + A_j N_j,$$

and

$$X_2 = \frac{a_j X_1 + b_j Y_1 + c_j}{f_j X_1 + g_j Y_1 + h_j}, \quad Y_2 = \frac{p_j X_1 + q_j Y_1 + r_j}{f_j X_1 + g_j Y_1 + h_j}. \tag{18}$$

All of the coefficients will be dtermined from observation at a single station. The solution may therefore be obtained from data of more than two stations by a graphical method or probably by the method of least squares.

(3) *Cone-type*

Some theoretical studies on the focal mechanism of a cone-type have been made, as stated before. In most of these cases, the radial and tangential displacements at a great distance compared with the wavelength are exactly or approximately expressed in the following form involving spherical harmonics ;

$$\left. \begin{array}{l} u_r = \dfrac{A}{r} [a_0 P_0(\cos \theta) + a_2 P_2(\cos \theta)] \exp\{i\omega(t - r/a)\} \\[3mm] u_\theta = \dfrac{B}{r} \dfrac{d}{d\theta} [a_0 P_0(\cos \theta) + a_2 P_2(\cos \theta)] \exp\{i\omega(t - r/b)\} \\[3mm] u_\varphi = 0 . \end{array} \right\} \tag{19}$$

Let us consider the geographical co-ordinate (r, Θ, Φ), taking the x-axis northward, the y eastward and the z upward. If we denote the angle of inclination of the polar axis by ψ, and the azimuth of it measured clockwise from northward by β, the two co-ordinate systems are connected by ;

$$\cos \theta = \sin \Theta \cos \psi \cos (\Phi - \beta) + \cos \Theta \sin \psi \tag{20}$$

and we have

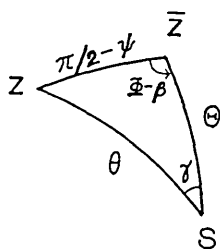$$\frac{\sin \theta}{\sin (\Phi - \beta)} = \frac{\sin (\pi/2 - \psi)}{\sin \gamma} \tag{21}$$

Fig. 4.

from spherical trigonometry with the aid of Fig. 4. Θ and Φ are defined as in the foregoing sections.

The displacement components u_Θ and u_Φ are transformed from u_θ and u_φ in a general form, that is, $u_\Theta = u_\theta \cos \gamma - u_\varphi \sin \gamma$, $u_\Phi = u_\theta \sin \gamma + u_\varphi \cos \gamma$. In the present case, however, the amplitudes of SV

and SH waves are related only to u_θ as follows, because $u_\varphi = 0$;

$$u_\Theta = u_\theta \cos \gamma , \quad u_\Phi = u_\theta \sin \gamma , \quad \text{or} \quad h_3 = \tan \gamma . \qquad (22)$$

Combining Eqs. (19), (20), (21) and (22), we have a quadratic equation similar to Eq. (18) for double couples, if we put $\tan \beta = X$ and $\sec \beta \tan \psi = Y$. That is,

$$\left.\begin{aligned} Y^2 + P_j(X)Y + Q_j(X) &= 0 \\ P_j(X) = u_j X + v_j , \quad Q_j(X) &= \alpha_j X^2 + \beta_j X + \gamma_j \end{aligned}\right\} \qquad (23)$$

where

$$u_j = -2 \cot \Theta_j \sin \Phi_j , \quad v_j = -2 \cot \Theta_j \cos \Phi_j ,$$

$$\alpha_j = (\cos^2 \Theta_j \sin^2 \Phi_j - h_{3j}^2 \cos^2 \Phi_j)/\sin^2 \Theta_j ,$$

$$\beta_j = 2 \sin \Phi_j \cos \Phi_j (h_{3j}^2 + \cos^2 \Theta_j)/\sin^2 \Theta_j ,$$

$$\gamma_j = (\cos^2 \Theta_j \cos^2 \Phi_j - h_{3j}^2 \sin \Phi_j)/\sin^2 \Theta_j$$

X and Y may be solved from data of more than two stations, in the same way as described before. Moreover, the angle of vertex of nodal cone 2α will be estimated from the following relation, based on Eq. (19).

$$\left.\begin{aligned} \cos 2\alpha &= \frac{C_1 \sin 2\theta_1 \cos 2\theta_2 - C_2 \sin 2\theta_2 \cos 2\theta_1}{C_1 \sin 2\theta_1 - C_2 \sin 2\theta_2} \\ C_j &= h_{2j}/\sqrt{1 + h_{3j}^2} . \end{aligned}\right\} \qquad (24)$$

In all of the three types of mechanism, dynamic parameters representing the source mechanism will be obtained from two of the three amplitude ratios, at a single station data for single couple case, or at two stations data for double couples and a cone-type, when the focus is located.

3. Effects of Crustal Structure

Seismic waves emitted from a focus suffer considerable change in their amplitudes and direction of the ray paths from refraction and reflection, during the travelling through discontinuity surfaces within the earth's crust to an observation station on the ground surface, when the wave period is short as compared with the layer thickness. It is, therefore, required first to eliminate these effects, so that we may deduce a focal mechanism from recorded amplitudes at the station, determining the displacements and the direction of emergence at the focus.
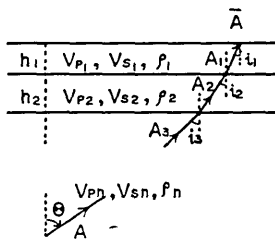
Fig. 5.

Assuming a horizontally layered structure as shown in Fig. 5, we denote the original amplitude by A, the one in each layer by A_k, and horizontal and vertical components of the surface amplitude by $\overline{A}_{(H)}$ and $\overline{A}_{(r)}$. Let the emergent angle be Θ, the angle of incidence to each layer be i_k, the velocities in the layer V_k, and the density of the medium ρ_k. We then have,

$$V_{P_k}/\sin i_{P_k} = V_{P_n}/\sin \Theta_P = V_{S_k}/\sin i_{S_k} = V_{S_n}/\sin \Theta_S \,,$$

$$(k=1, 2, \cdots, n) \quad (25)$$

the suffixes p and s indicating the quantity belonging to the P and S waves. The curvature of the ray path will be determined by Eq. (25). On the other hand, the relations between the above denoted amplitudes can be expressed in the following forms for the P, SV and SH waves, respectively.

$$\left.\begin{array}{lll} \overline{A}_{P(H)}/A_{P_1}=f_1(i_{P_1})\,, & \overline{A}_{P(r)}/A_{P_1}=f_2(i_{P_1})\,, & A_{P_{k-1}}/A_{P_k}=F_k(i_{P_k}) \\ \overline{A}_{SV(H)}/A_{SV_1}=g_1(i_{S_1})\,, & \overline{A}_{SV(r)}/A_{SV_1}=g_2(i_{S_1})\,, & A_{SV_{k-1}}/A_{SV_k}=G_k(i_{S_k}) \\ \overline{A}_{SH}/A_{SH_1}=2\,, & & A_{SH_{k-1}}/A_{SH_k}=H_k(i_{S_k}). \end{array}\right\} \quad (26)$$

If we suppose propagation of the plane waves, these functions can be calculated by the following formulae (Ewing et al., 1957).

$$\left.\begin{array}{l} F_k(i_{P_k})=\dfrac{2(m_2+m_4)}{(l_1+l_3)(m_2+m_4)-(l_2+l_4)(m_1+m_3)} \\[3mm] G_k(i_{S_k})=\dfrac{2(l_1+l_3)}{(l_1+l_3)(m_2+m_4)-(l_2+l_4)(m_1+m_3)} \\[3mm] H_k(i_{S_k})=\dfrac{2}{1+\mu_{k-1}\cot i_{S_{k-1}}/\mu_k \cot i_{S_k}} \end{array}\right\} \quad (27)$$

where

$$l_1=\rho_{k-1}/\rho_k+q\,, \qquad\qquad m_4=\rho_{k-1}/\rho_k+q$$

$$l_2=\tan i_{S_k}(1-\rho_{k-1}/\rho_k-q)\,, \qquad m_3=-\tan i_{P_k}(1-\rho_{k-1}/\rho_k-q)$$

$$l_3=\tan i_{P_k}\cot i_{S_{k-1}}(1-q)\,, \qquad m_2=\tan i_{S_k}\cot i_{S_{k-1}}(1-q)$$

$$l_4=-\cot i_{P_{k-1}}\cdot q\,, \qquad\qquad m_1=\cot i_{S_{k-1}}\cdot q$$

$$q=k(V_{S_k}/V_{P_k})^2 \sin^2 i_{P_k}=k\sin^2 i_{S_k}\,,$$

$$k=2[1-(V_{S_{k-1}}/V_{S_k})^2(\rho_{k-1}/\rho_k)]\,.$$

While, $f_i(i_{P_1})$ and $g_i(i_{S_1})$ have already been obtained as a parameter of Poisson's ratio, by Matuzawa (1932) and Knopoff and others (1957). All of the functions, f_i, g_i, F_k, G_k and H_k can be computed in terms of the emergent angle at the focus using Eq. (25). It is to be remarked here that these formulae should be somewhat modified when the angle of incidence of the S waves is over the critical angle. But they are of less use because it seems rather inadequate to analyse the data under these circumstances, owing to non-linear particle motion of S (Nuttli, 1961).

If Poisson's ratios of the respective media are nearly the same, both P and S waves travel along the same path, i. e. $\Theta_P = \Theta_S$ and $i_{P_k} = i_{S_k}$. When we discuss the amplitude ratios of P, SV and SH waves observed at a station in such a case, the decrease in their amplitudes due to travel distance may be omitted, neglecting difference between the attenuation of the waves. The ratios of the surface amplitude to the amplitude in a homogeneous medium are written as follows;

$$\begin{aligned}
\overline{A}_{P(H)}/A_P &= f_1 F_1 F_2 \cdots F_n = F_H(\Theta) , & \overline{A}_{P(V)}/A_P &= f_2 F_1 F_2 \cdots F_n = F_V(\Theta) \\
\overline{A}_{SV(H)}/A_{SV} &= g_1 G_1 G_2 \cdots G_n = G_H(\Theta) , & \overline{A}_{SV(V)}/A_{SV} &= g_2 G_1 G_2 \cdots G_n = G_V(\Theta) \\
\overline{A}_{SH}/A_{SH} &= 2H_1 H_2 \cdots H_n = H(\Theta) . &
\end{aligned} \right\} \quad (28)$$

In the present study, the data observed at three stations of the Earthquake Research Institute in the southern Kwanto region—Tsukuba, Inubô and Nokogiriyama—was used for our purpose. Crustal structure near the regions are presumed as illustrated in Fig. 6 from the results
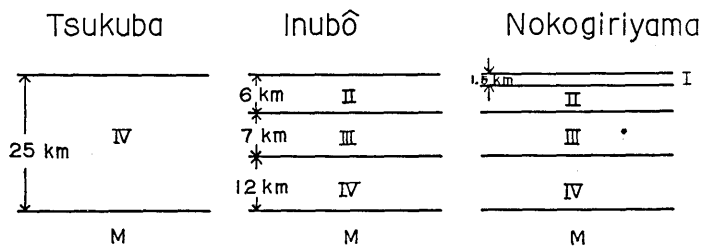

Fig. 6. Crustal structure.

	Vp	Vs	ρ
I	2.0 km/sec	1.1 km/sec	2.00
II	4.9	2.9	2.55
III	5.6	3.3	2.70
IV	6.1	3.6	2.80
M	7.7	4.5	3.25

of explosions and seismic prospectings (Usami et al., 1958 ; Res. Group for Expl. Seism., 1958 ; Asano et al., 1959 ; Tateishi et al., 1956, 1958).

Fig. 7. Relation between the emergent angle and the angle of incidence to each layer.

Densities were determined from an empirical density versus seismic velocity curve compiled by Nafe and Drake (unpublished ; cited by Talwani et al., 1959).

Fig. 7 shows the relation between the emergent angle Θ and the incident angle i_k to each layer, and Fig. 8 the ratio of the horizontal component of surface amplitude to the vertical one. The transmission rates F_k, G_k and H_k of the P, SV and SH waves computed for the presented structure are shown in Fig. 9. We can find in Figs. 10, 11 and 12 the ratios of the surface amplitude at each station

(a) P waves

(b) SV waves

Fig. 8. Relation between the horizontal and vertical components of surface amplitude.

to the original amplitudes for the three kinds of waves. The displacement amplitudes in a homogeneous earth may be estimated from these graphs, if their decrease due to the travel distance is not taken into consideration.

(a) *P* waves

(b) *SV* waves

(c) *SH* waves]
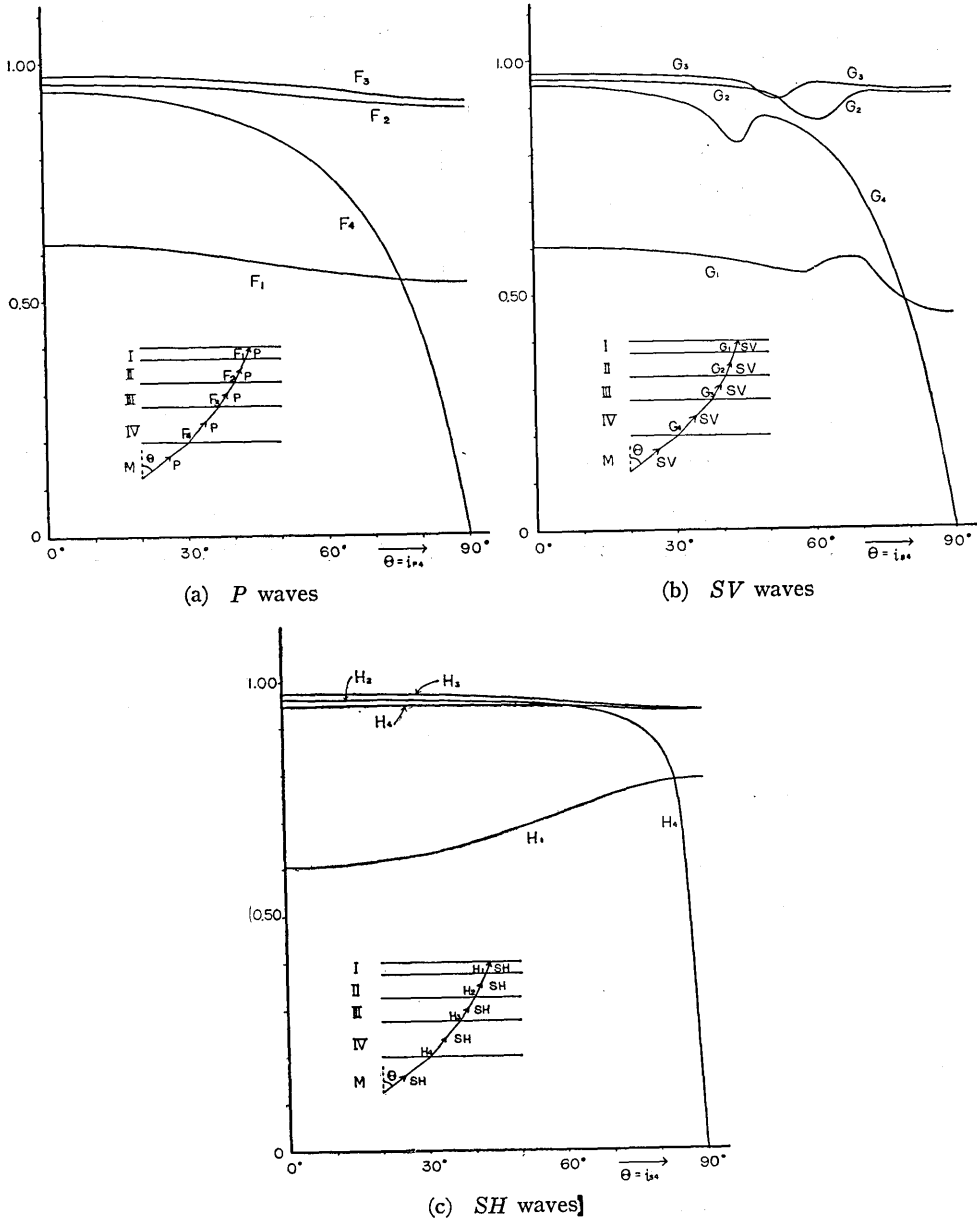
Fig. 9. Transmission rates of the incident waves at each interface.

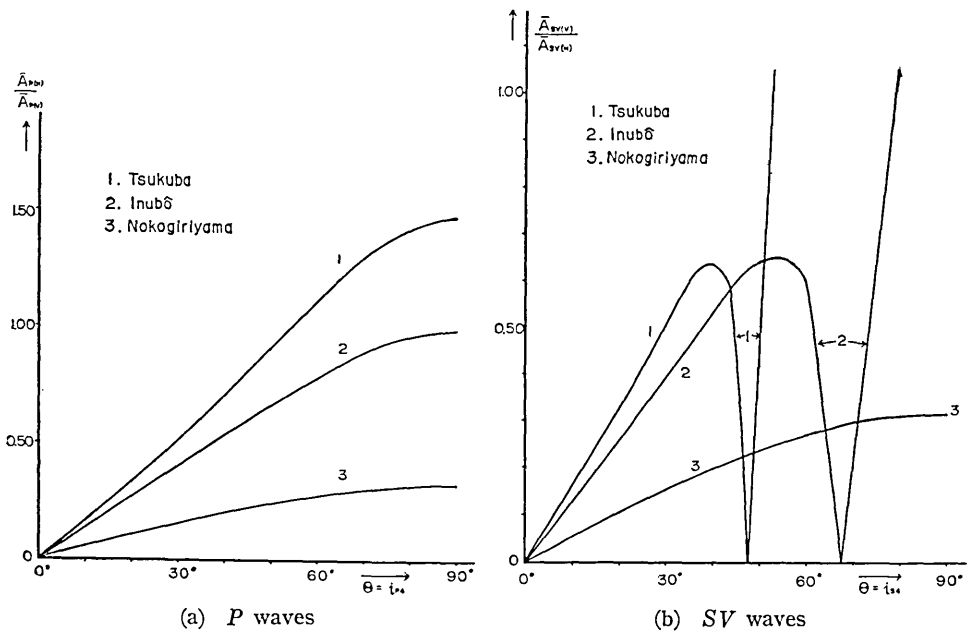(a) *P* waves   (b) *S* waves
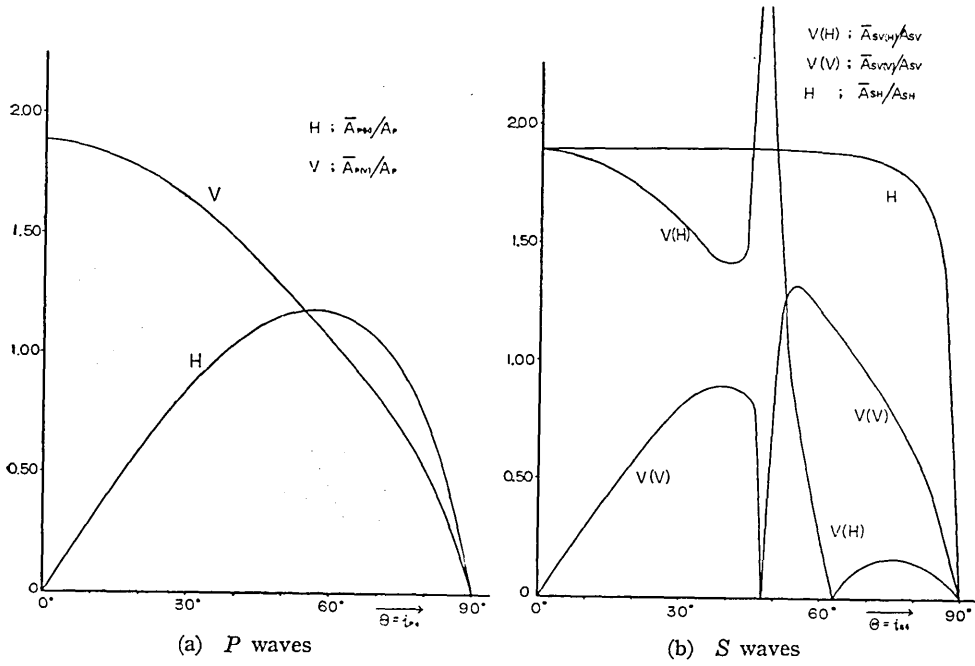
Fig. 10. Ratio of the surface amplitude at Tsukuba to the original amplitude.

(a) *P* waves   (b) *S* waves
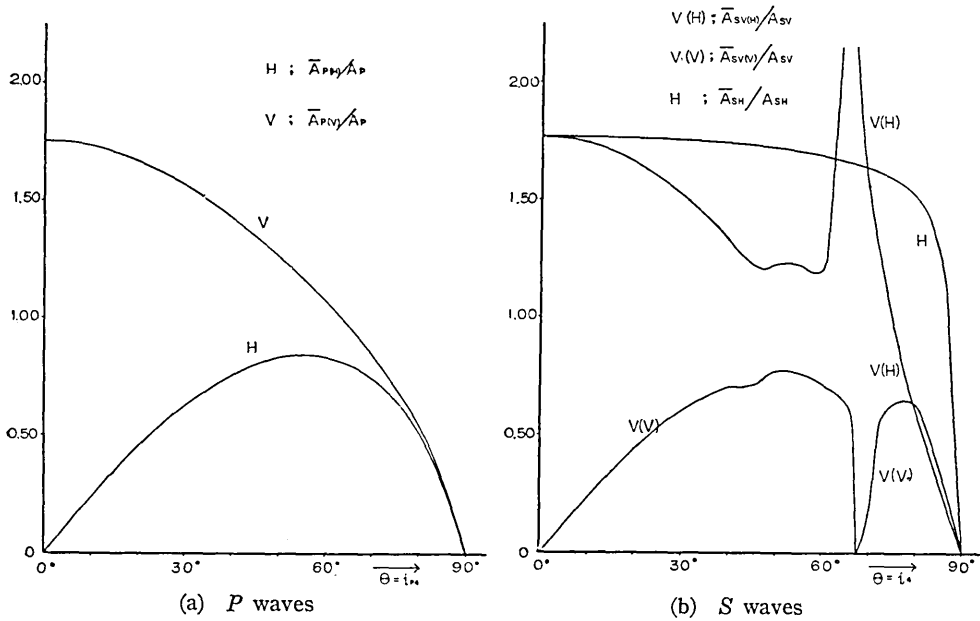
Fig. 11. Ratio of the surface amplitude at Inubô to the original amplitude.

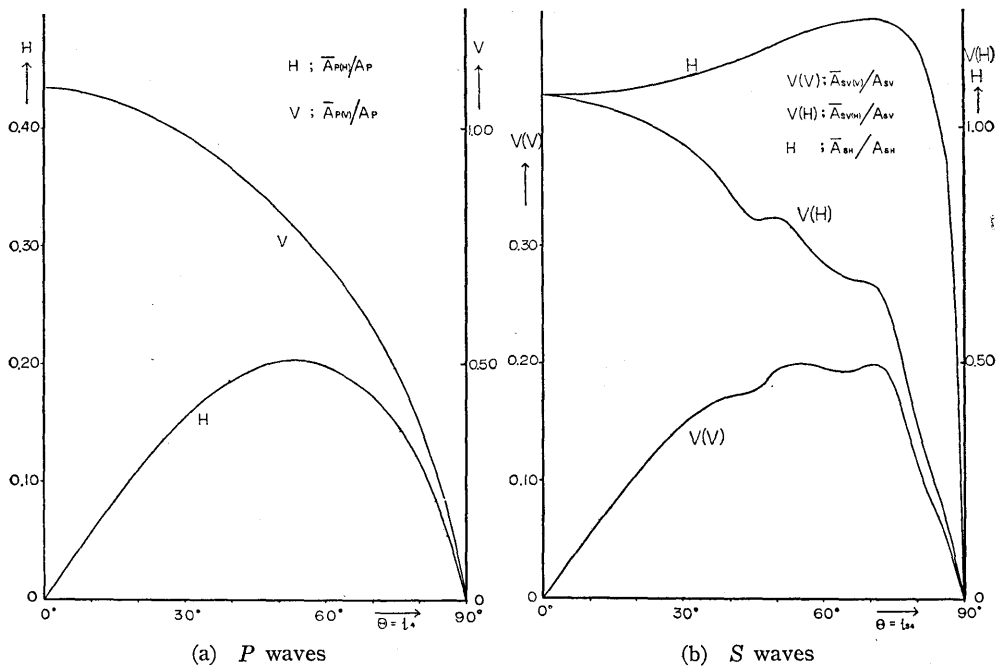(a) *P* waves   (b) *S* waves

Fig. 12. Ratio of the surface amplitude at Nokogiriyama to the original amplitude.

4. Observed Data

In this study, seismograms were analysed which were recorded with electromagnetic seismographs of *HES* type at Tsukuba, Inubô and Nokogiriyama. The free period of both the pendulum and galvanometer is 1 sec and both are critically damped. Maximum magnification is roughly estimated to be 30,000 at Tsukuba, 11,000 at Inubô and 3,000 at Nokogiriyama. The film speed is about 9 cm/min on its reader. Among a great many earthquakes observed during the period from July, 1961 to March, 1962, 10 local earthquakes were selected for the present purpose, in which all components of both *P* and *S* wave motions were clearly recorded at the said three stations. Observed data for these earthquakes are tabulated in Table 1. The recorded amplitudes are associated with the first motions of *P* and *S* waves, and are corrected by magnification of each component.

The foci of the 10 earthquakes could be located graphically, using the *P*–*S* times at the three stations, as shown in Fig. 13. This was done with the aid of a diagram of isochronic lines of *P*–*S* times, constructed

Table 1.

Shock No.	Date	St.	Commence-ment time	P-S (sec)	$\overline{A}_{P(E)}$	$\overline{A}_{P(N)}$	$\overline{A}_{P(V)}$	$\overline{A}_{S(E)}$	$\overline{A}_{S(N)}$	$\overline{A}_{S(V)}$
	1961		h m s							
J-494	July 19	T	16 24 02	9.8	− 1.0	8.0	12.6	121.0	145.5	−98.1
		I		9.8	1.1	0.5	1.9	14.5	−33.4	−17.1
		N		9.6	1.0	2.8	−12.8	− 5.5	− 9.7	− 6.9
J-502	July 19	T	18 19 55	23.0	16.0	4.0	− 9.8	−24.0	−39.5	−52.6
		I		23.1	2.0	3.2	− 8.5	−14.0	−15.3	−25.6
		N		32.3	1.0	0.5	− 2.0	6.5	2.8	1.5
A-231	Aug. 15	T	01 45 00	8.0	− 1.5	− 3.5	− 5.1	−22.0	−29.0	3.9
		I		11.0	1.4	− 0.5	2.8	−11.0	6.3	6.1
		N		11.0	0.5	0.7	− 2.0	4.5	7.4	4.9
S- 32	Sep. 3	T	00 38 38	8.2	2.5	21.0	33.8	41.0	−53.5	86.4
		I		10.0	6.5	1.4	5.7	−20.0	−23.4	19.0
		N		7.1	0.2	0.7	− 2.0	− 7.0	9.2	6.4
S-139	Sep. 9	T	18 16 44	20.1	1.5	2.0	3.1	−12.5	12.5	28.3
		I		25.0	10.5	3.6	5.7	−11.0	−12.2	28.4
		N		17.3	− 0.7	1.4	6.9	− 1.0	12.4	3.9
O-133	Oct. 11	T	17 55 05	10.5	−11.5	1.0	−16.1	39.0	46.0	−18.8
		I		17.1	2.0	− 1.4	3.8	−20.0	9.0	4.0
		N		16.6	− 0.8	1.5	− 4.9	−10.0	−24.0	− 3.9
O-317	Oct. 25	T	03 59 37	8.2	1.5	14.0	21.2	8.0	−87.0	25.1
		I		10.9	2.0	− 3.2	6.6	30.0	10.4	− 7.6
		N		10.6	− 0.2	− 2.0	1.8	6.0	14.0	3.9
N-348	Nov. 29	T	21 56 10	9.2	− 0.8	3.0	3.9	−23.0	−10.0	− 9.4
		I		5.7	− 3.5	− 0.9	− 5.2	4.0	− 3.6	3.3
		N		9.2	− 0.3	− 0.4	2.9	6.5	3.7	3.7
D-349	Dec. 28	T	21 09 12	9.2	1.5	4.0	5.1	−19.0	−32.5	14.1
		I		10.2	− 0.4	− 0.2	− 8.5	4.0	2.7	− 5.2
		N		9.0	0.1	0.8	− 4.4	6.0	− 4.6	− 1.0
D-358	Dec. 29	T	12 26 09	9.7	0.3	1.5	2.8	− 9.0	− 4.0	24.7
		I		12.0	0.9	0.3	4.3	− 2.5	3.6	2.8
		N		8.6	− 0.2	0.5	− 2.8	−13.0	5.8	3.9

Table 2.

Shock No.	$\varDelta$ (km)			Θ			$\varPhi$			h (km)
	T	I	N	T	I	N	T	I	N	
J-494	65.0	62.8	60.3	47°.5	47°.5	45°.5	355°.0	81°.5	210°.5	68
J-502	225.0	227.5	327.5	83.5	84.0	86.0	229.0	207.0	217.0	47
A-231	41.5	81.8	78.0	36.5	58.0	56.0	17.0	101.5	189.0	63
S- 32	67.0	82.5	52.0	90.0	90.0	90.0	12.5	82.0	190.5	25
S-139	184.5	238.0	150.5	73.0	78.0	69.0	65.5	85.0	105.5	73
O-133	63.8	148.5	139.5	41.5	68.0	65.5	106.5	120.0	164.5	79
O-317	45.5	79.3	74.0	39.0	58.0	53.5	13.0	98.0	190.5	63
N-348	77.8	37.2	74.5	90.0	90.0	90.0	333.5	61.0	232.0	25
D-349	63.0	75.0	56.8	51.0	57.5	47.5	6.0	84.5	198.5	60
D-358	70.5	95.8	51.5	54.0	64.0	45.0	22.5	84.0	176.5	60

by Kayano (unpublished) based on the presented structure. Table 2 summarises the determined values of the epicentral distance, azimuth and emergent angle, each referring to the respective stations, and of the focal depth.

Focal depths in most of the shocks treated here are from 60 km to 70 km exept in two earthquakes. The emergent angle in the case of these deeper earthquakes was slightly corrected, under an assumption that the velocity of *P* waves in the earth's mantle increases from 7.7 km/sec beneath the Moho-discontinuity to 8.0km/sec at the depth of about 50 km, and that of *S* waves increases at the same rate.
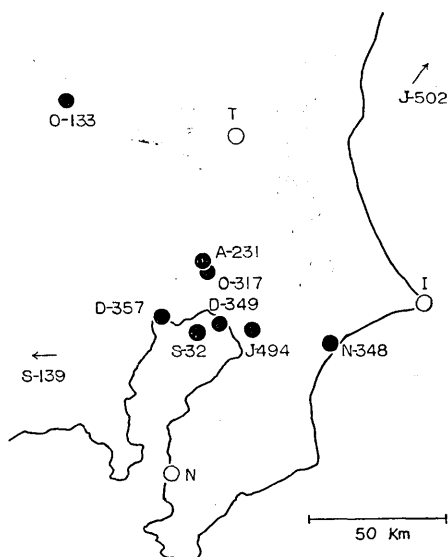

Fig. 13. Location of observation stations and epicentres of the earthquakes mentioned.

5. Calculated Results

The amplitude ratios of the three kinds of waves in the case of a homogeneous medium, $h_1 = A_P/A_{SV}$, $h_2 = A_P/A_{SH}$ and $h_3 = A_{SV}/A_{SH}$, which were computed from the observed displacements by means of the graphs in Figs. 10–12, are listed in Table 3. A_P and A_{SV} are obtainable independently from the recorded horizontal or vertical component of the surface amplitude. The two components can be checked by their ratio depending upon the emergent angle, shown in Fig. 8, but the observed ratios do not always agree satisfactorily with the expected values. This may probably be due to errors resulting from the measurement of somewhat less reliable horizontal amplitude in *P* waves and vertical in *S* wave, when a low velocity layer overlies crustal layers. Such being the case, the better recorded component was employed in determining the original amplitudes.

Making use of the values listed in Tables 2 and 3, all of the coefficients in Eqs. (9), (17) and (23) can be determined, but are too many to list. Eq. (9) for a single couple can easily be solved from data of a single station, so that three sets of solutions are plotted respectively as a point on the (X, Y) graph mentioned in the foregoing theory. On

T. MIKUMO

Table 3.

Shock No.	St.	h_1	h_2	h_3
J-494	T	-0.177 ± 0.007	0.134 ± 0.005	-0.758 ± 0.011
	I	-0.131 ± 0.070	0.094 ± 0.020	-0.716 ± 0.347
	N	0.944 ± 0.131	90.991 ± 45.500	96.110 ± 48.055
J-501	T	0.072 ± 0.004	3.149 ± 0.337	43.600 ± 3.970
	I	0.413 ± 0.149	-5.627 ± 0.605	-13.632 ± 1.583
	N	-0.292 ± 0.057	2.893 ± 0.725	-9.921 ± 1.954
A-231	T	-0.134 ± 0.012	0.324 ± 0.036	-2.425 ± 0.192
	I	0.235 ± 0.020	-1.017 ± 0.170	-4.330 ± 0.689
	N	-0.247 ± 0.046	0.935 ± 0.253	-3.778 ± 0.757
S-32	T	0.389 ± 0.013	3.952 ± 0.121	10.158 ± 0.428
	I	0.222 ± 0.028	1.255 ± 0.160	5.643 ± 0.485
	N	-0.218 ± 0.042	-1.494 ± 0.025	6.880 ± 0.810
S-139	T	0.119 ± 0.034	-0.474 ± 0.087	-3.975 ± 0.444
	I	0.548 ± 0.092	1.312 ± 0.230	2.397 ± 0.417
	N	-1.841 ± 0.181	1.193 ± 0.065	-0.648 ± 0.061
O-133	T	1.030 ± 0.092	0.358 ± 0.015	0.347 ± 0.028
	I	0.349 ± 0.019	3.054 ± 0.793	8.762 ± 2.165
	N	0.255 ± 0.036	-0.597 ± 0.093	-2.340 ± 0.220
O-317	T	0.241 ± 0.005	0.963 ± 0.038	3.987 ± 0.148
	I	-0.250 ± 0.027	-0.702 ± 0.098	2.804 ± 0.283
	N	0.118 ± 0.020	-0.809 ± 0.217	-6.827 ± 1.090
N-348	T	-1.621 ± 0.669	-0.946 ± 0.064	0.583 ± 0.221
	I	2.726 ± 0.905	-5.190 ± 0.746	-1.908 ± 0.729
	N	0.321 ± 0.049	-16.194 ± 2.295	-50.579 ± 7.480
D-349	T	0.184 ± 0.018	-0.499 ± 0.066	-2.710 ± 0.241
	I	2.169 ± 0.310	5.622 ± 1.341	2.593 ± 0.845
	N	1.707 ± 0.398	0.845 ± 0.100	0.495 ± 0.118
D-358	T	0.144 ± 0.082	-0.417 ± 0.188	-2.892 ± 0.613
	I	4.515 ± 0.681	4.406 ± 0.355	0.976 ± 0.178
	N	-0.401 ± 0.184	-0.439 ± 0.097	1.094 ± 0.172

the contrary, Eq. (17) for double couples and Eq. (23) for the cone-type were solved graphically. On the same graph a set of curves of the second degree corresponds to an observation at one station. Data from the three stations give three sets of solutions by intersection of each pair of the curves. Fig. 14 shows an example of the graph for the three types of the mechanism.

For the sake of easy comparison of the results, the solutions in the (X, Y) graph are translated into those in the (β, ψ) graph as illustrated in Fig. 15, in which the azimuth β is given as an angle measured clockwise from an upward directed axis and ψ as a radial length. The extent of scattering of the plotted points may offer a clue to the estimation as to what type of force system is best fitted to the observed results. Theoretically, the problem can also be solved by the method of
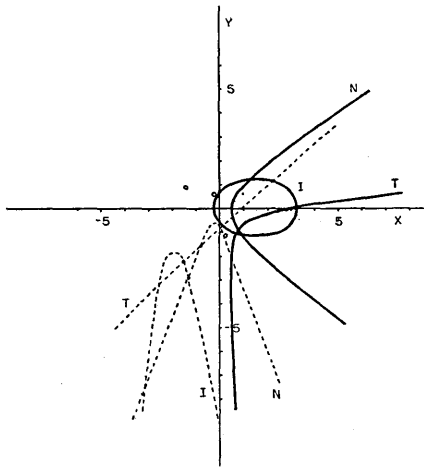
Fig. 14. The (X, Y) graph.
$(X=\tan \beta, \ Y=\sec \beta \tan \psi)$
The solid lines correspond to the case of double couples, the broken line to cone type and the dots to a single couple case.
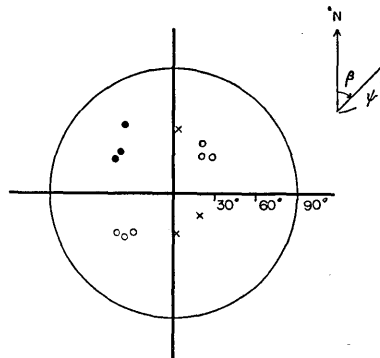

Fig. 15. The (β, ψ) graph.
$(\beta;$ azimuth, $\psi;$ inclination)
The open circles, solid circles and crosses correspond to the case of double couples, cone-type and a single couple, respectively.

Table 4.

Shock No.		Double Couples		Cone-type		
		Strike	Dip	Strike	Dip	Vertical Angle
J-494	I	N61.9$\pm$ 2.4E	10.6$\pm$ 2.3NE	N28.4$\pm$0.7E	8.0$\pm$1.3SW	
	II	N35.9$\pm$ 4.3W	35.6$\pm$21.2NW			
J-502	I	N46.2$\pm$ 8.9W	44.9$\pm$ 2.5NW			
	II	N46.3$\pm$ 8.9W	45.1$\pm$ 1.7SE			
A-231	I	N21.4$\pm$ 8.1W	21.0$\pm$ 5.5NW			
	II	N56.1$\pm$22.8E	29.6$\pm$20.7SW			
S- 32	I	N25.0$\pm$ 7.9W	32.3$\pm$11.1SE			
	II	N35.2$\pm$17.5E	38.2$\pm$14.0NE			
S-139	I	N 2.2$\pm$ 3.7W	52.6$\pm$ 2.8SE	N59.1$\pm$1.0E	32.1$\pm$1.5SW	68.6$\pm$ 1.5
	II	N26.4$\pm$20.8W	33.8$\pm$ 5.3NW			
O-133	I	N39.2$\pm$ 6.6E	38.9$\pm$ 3.8NE	N50.2$\pm$8.0W	57.1$\pm$6.7NW	84.2$\pm$21.4
	II	N55.3$\pm$ 7.3E	50.0$\pm$ 3.0SW			
O-317	I	N60.3$\pm$ 0.5E	5.9$\pm$ 0.5SW			
	II	N35.5$\pm$ 6.8W	44.3$\pm$14.9SE			
N-348	I	N19.3$\pm$ 2.5E	12.0$\pm$ 8.6NE	N48.5$\pm$2.9E	25.7$\pm$5.0SW	
	II	N69.4$\pm$ 2.2W	5.8$\pm$ 5.0NW			
D-349	I	N43.4$\pm$ 5.0E	6.6$\pm$ 5.4SW	N44.5$\pm$6.0E	50.1$\pm$4.6NE	
	II	N43.7$\pm$ 0.9W	23.5$\pm$12.5NW			
D-358	I	N32.7$\pm$ 6.1W	13.5$\pm$ 5.2NW	N32.4$\pm$8.6E	12.1$\pm$7.8NE	78.8$\pm$22.2
	II	N13.8$\pm$ 7.2E	71.2$\pm$ 5.6SW			

least squares when data are obtained at more stations. It may safely be said of the above example that the focal mechanism of the earthquake cited is of double couples rather than cone-type or single couple.

Table 4 summarises the final results estimated for the 10 earthquakes. The strike and dip correspond to β and φ. The errors contained in the results indicate an average of deviation from the mean value of three sets of the solutions. The cumulative error resulting from errors accompanied by measurements of surface amplitudes, the P–S times and of Θ and Φ, is evaluated as being within the above range.

6. Discussion

The calculated results are as shown in Table 4. Satisfactory solutions could not be obtained under the assumption of a single couple for all of the earthquakes treated here. The double couples, on the contrary, agreed fairy well with the observed data, allowing a certain degree of error. To only one earthquake (No. S–139) the mechanism of cone-type, rather than of double couples, may be considered to fit slightly better. Although we cannot come to a definite conclusion on account of insufficient data, we may be allowed to consider that the double couples are more promising than the other two systems for the above-mentioned earthquakes, as far as the present data are concerned.
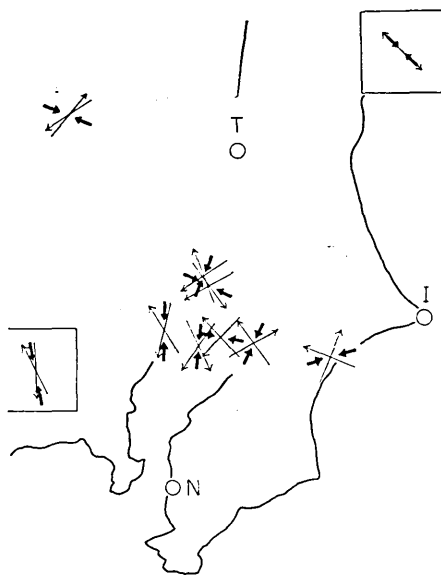

Fig. 16. Distribution of the force directions (thin arrows) and horizontal component of maximum pressures (thick arrows). Thin arrows indicates the direction of downward force.

Fig. 16 indicates the distribution of force directions and of horizontal component of maximum pressures deduced from the sense of first motion at the three stations, assuming the mechanism to be of double couples. No systematic pattern is recognized in this figure. This trend shows only a little difference from the results for greater earthquakes (probably $4 < M < 7$), that occurred in the same area, which were derived by Ichikawa (1961)

from distribution of P wave motions based on usual way. It may however be said that the mechanism itself of local earthquakes of very small magnitude ($1 < M < 3$) in the southern Kwanto region, which is supposed to be of double couples, does not differ greatly from that of larger earthquakes in the same district. It contrasts sharply with that of local earthquakes with the same order of magnitude taking place in the upper crust in Wakayama region (Mikumo, 1959). This seems to raise question on local eartquake mechanism.

The adopted method may involve some problems to be solved, and the results should be compared with those obtained by other methods. But it is of practical use for the determination of focal mechanism from data of a few stations, only if technical difficulties relating to the problems are overcome.

Acknowledgement

References

W. M. ADAMS, A study of earthquake mechanism using S wave data, *Bull. Seism. Soc. Amer.*, **48** (1958), 201–209.

L. M. BALAKINA, E. F. SAVARENSKY and A. V. VVEDENSKAYA, On determination of earthquake mechanism, *Phys. and Chem. of the Earth*, **4** (1961), 211–238.

E. N. BESSONOVA, O. D. GOTSAZE, V. I. KEYLIS-BOROK, S. D. KOGAN, L. N. MALINOVSKAYA et al., Investigation of the mechanism of earthquakes, *Trudy, Geofiz. Inst., Akad. Nauk, SSSR, 40; Soviet research in Geophysics in English translation*, **4** (1960).

P. BYERLY, A. I. MEI and C. ROMNEY, Dependence on azimuth of the amplitudes of P and
    PP, *Bull. Seism. Soc. Amer.*, **39** (1949), 291-298.

P. BYERLY, Nature of faulting as deduced from seismograms, Crust of the Earth, *Geol. Soc.
    Amer.*, Special Paper, **62** (1955), 75-85.

P. BYERLY and W. V. STAUDER, Motion at the source of an earthquake, Pub. Dominion
    Obs. Ottawa, (1958), 255-261.

J. H. HODGSON and R. S. STOREY, Tables extending Byerly's fault-plane technique to earth-
    quakes of any focal depth, *Bull. Seism. Soc. Amer.*, **43** (1953), 49-61.

J. H. HODGSON, Nature of faulting in large earthquakes, *Bull. Geol. Soc. Amer.*, **63** (1957),
    611-644.

H. HONDA, On the amplitude of *P* and *S* waves of deep earthquakes, *Geophys. Mag.*, **8**
    (1934), 153-164; 327-332.

H. HONDA, A. MASATSUKA and K. EMURA, On the mechanism of the earthquakes and
    stresses producing them in Japan and its vicinity, Sci. Rep. Tôhoku Univ., Ser. 5,
    Geophys. **4** (1952), 42-60; **8** (1956), 186-205.

H. HONDA, The mechanism of the earthquakes, Sci. Red. Tôhoku Univ., Ser. 5, *Geophys.*
    9 (1952).

M. ICHIKAWA, A study of occurrence mechanism of an earthquake on Oct. 26, 1952, using
    P and *S* waves (in Japanese), *Quart. Journ. Seism.*, **23** (1959), 135-148.

M. ICHIKAWA, On the mechanism of the earthquakes in and near Japan during the period
    from 1950 to 1957, *Geophys. Mag.*, **30** (1961), 355-403.

R. E. INGRAM, Generalized focal mechanism, Pub. Dominion Obs. Ottawa, **24** (1960), 305-
    308.

W. INOUYE, Notes on the origin of earthquake, *Bull. Earthq. Res. Inst.*, **14** (1936), 582-
    598; **15** (1938) 956-964.

M. ISHIMOTO, Existence d'une source quadruple au foyer sismique d'apres l'étude de la
    distribution des mouvements initiaux des secousses sismique, *Bull. Earthq. Res.
    Inst.*, **10** (1932), 449-471.

H. KAWASUMI, Study on the propogation of seismic waves (2nd Paper), *Bull. Earthq. Res.
    Inst.*, **11** (1933), 403-453; **12** (1934), 660-705.

V. I. KEYLIS-BOROK, Methods and results of the investigation of earthquake mechanism,
    Travaux Scientifiques, **19** (1956), 384-394.

V. I. KEYLIS-BOROK, The determination of earthquake mechanism, using both longitudinal
    transversal waves, Ann. di Geofisica **10** (1957), 105-128.

V. I. KEYLIS-BOROK, Some new investigations of earthquake mechanism, Pub. Dominion
    Obs. Ottawa **24** (1960), 335-341.

L. KNOPOFF and F. GILBRT, Radiation from a strike-slip fault, *Bull. Seism. Soc. Amer.*,
    49 (1959), 163-178.

L. KNOPOFF and F. GILBRT, First motions from seismic sources, *Bull. Seism. Soc. Amer.*,
    50 (1960), 117-134.

T. MATUZAWA, On the relative magnitude of the preliminary and the principal motion of
    earthqeake motions, *Jap. Journ. Astr. and Geophys.*, **4** (1962), 1-33.

T. MIKUMO, A consideration on generation mechanism of local earthquakes, *Mem., Coll.
    Sci. Kyoto Univ.*, Ser. A, **29** (1959), 221-240.

H. NAKANO, Notes on the nature of the focus which gives rise to the earthquake motions,
    Seism. Bull. Centr. Meteor. Obs., Japan, **1** (1923), 92-120.

A. R. RITSEMA, On the use of transverse waves in earthquake mechanism studies and the
    direction of fault-displacement in southeast Asia earthquakes, *Meteorol. and Geophys.*

Inst., Djakarta, Verhandelingen 52 (1957).

H. J. SCHAEFFNER, Die Grundlagen und Answertverfahren zur seismischen Bestimmung von Erdbebenmechanismen, Freiberger Forschungshefte, C 63 (1959).

A. E. SCHEIDEGGER, The geometrical representation of fault-plane solutions of earthquakes, *Bull. Seism. Soc. Amer.*, **47** (1957), 89-110.

W. STAUDER, *S* waves and focal mechanism: the state of the question, *Bull. Seism. Soc. Amer.*, **50** (1960), 333-346.

W. STAUDER and W. M. ADAMS, A comparison of some *S*-wave studies of earthquake mechanism, *Bull. Seism. Soc. Amer.*, **51** (1961), 277-292.

S. TAKAGI, On the origin of earthquake, *Quart. Journ. Seism.*, C. M. O., (1953), 14-3, 1; 17-3, 1; 17-4, 53. (in Japanese)

T. USAMI and T. HIRONO, Elastic waves from a spheroidal cavity whose wall is subjected to normal stress of harmonic type, *Pap. in Met. and Geophys.*, **7** (1956), 288-321; *Geophys. Mag.*, **29** (1958), 11-36.

A. V. VVEDENSKAYA, The displacement field associated with rupture of continuity of an elastic medium, *Izv. Akad. Nauk.*, SSSR, ser. geofiz., **4** (1959), 516-526. (in English translation).

A. V. VVEDENSKAYA, Determination of the stresses acting in the earthquake sources based on observations at seismic stations, *Izv. Akad. Nauk.*, SSSR, ser. geofiz., **4** (1960), 513-519. (in English translation).

S. ASANO, N. DEN, T. MIKUMO, E. SHIMA and T. USAMI, On the travel-times of *S*-waves, derived from the explosion seismic observations, *Bull. Earthq. Res. Inst.*, **37** (1959), 279-306.

M. EWING, W. S. JARDETZKY and F. PRESS, Elastic waves in layered media (1957).

L. KNOPOFF, R. W. FREDRICK, A. F. GANGI and L. D. PORTER, Surface amplitudes of reflected body waves, *Geophys.*, (1957), 842-847.

T. MATUZAWA, An example of surface reflection of plane waves (in Japanese), *Zisin*, **4** (1932), 125-139.

O. NUTTLI, The effect of the earth's surface on the *S* wave particle motion, **51** (1961), 237-246.

RESEARCH GROUP FOR EXPLOSION SEISMOLOGY, Report on observation results of Chôshi explosion., *Rep. R. G. E. S.*, **16** (1958), 10-22. (in Japanese).

T. TATEISHI and K. HIRASAWA, Seismic prospecting in the vicinity of Yokoshiba Town, Chiba Prefecture, *Monthly Rep. Geol. Survey, Japan*, **8** (1957), 41-50. (in Japanese).

T. TATEISHI, On later phases observed in the Yokoshiba explosion, *Rep. R. G. E. S.*, **17** (1958), 11-19. (in Japanese).

T. USAMI, T. MIKUMO, E. SHIMA, I. TAMAKI, S. ASANO, T. ASADA and T. MATUZAWA, Crustal structure in northern Kwanto District by explosion seismic observations, *Bull. Earthq. Res. Inst.*, **36** (1958), 349-357.

19. 関東地方における微小地震の発震機構について

京都大学防災研究所 三 雲 健

発震機構についての研究は古くから多くの地震学者によつて盛んに行われて来た．しかしながら，これらの研究の多くは大きい地震に関するものであつて，小地震の場合には，広範囲の観測資料が得られにくいために，大きい地震の場合のように，初動分布や S 波の振動方向等の分布から節面を求めることが困難な場合が多い．筆者は，このような場合における 1 つの方法として，数観測点で記録される P 波と S 波の振幅比から，発震機構を推定することを試みた．まず，予想される発震型式として single couple, double couple, cone-type の 3 つの場合を仮定し，それぞれの場合において，このような力が働いた時の，無限弾性体中の遠距離における P 波，SV 波，SH 波の変位振幅を観測データの処理に便利な形に計算した．一方これらの波は，地殻中を通過して地表面の観測点へ到達するまでに，不連続面や地表面の影響等によつて，その振幅や経路に変化を受けるので，爆破地震動観測などの結果から定められた南関東地方の地殻構造についてこの影響を計算した．これを用いて，筑波，犬吠，鋸山において観測されたこれら 3 種の波の振幅比の補正を行ない次いで先の仮定により，震源に働いた力の方向（方位と地表面に対する傾斜）を推定した．観測点が 3 点以上あれば，どのような型式の発震機構が最も良く適合するかを見ることも原理的には可能である．南関東地方に起つた 10 個の微小地震の発震機構をこの方法によつて調べた結果，3 つの型式のうちでは double couple と思われる場合が多いが，資料が少ないので，明確な結論を下すには到らなかつた．